Desalination and Water Treatment
www.deswater.com

doi: 10.5004/dwt.2017.21596

95 (2017) 74–79
November

Effect of module configuration on the overall mass recovery in membrane distillation

Sagar Roy, Smruti Ragunath, Somenath Mitra*

Department of Chemistry and Environmental Science, New Jersey Institute of Technology, Newark, NJ 07102, USA, Tel. 001 (973) 5965611; emails: somenath.mitra@njit.edu (S. Mitra), sagar@njit.edu (S. Roy), sr262@njit.edu (S. Ragunath)

Received 25 July 2017; Accepted 28 October 2017

ABSTRACT

In spite of dramatic improvements in membrane properties, the overall mass recovery in membrane distillation (MD) remains quite low, and is a major drawback. In this paper, we present a comparative study on the effect of various module configurations on the overall mass recovery in MD. Experimental data with two modules with a heating stage show a water recovery enhancement of 38% and 96% compared with equivalent modules in series and parallel, respectively. A simulation with seawater and five modules in series with heating in between shows an increase in water recovery of 320% and brine concentration increases from 34,000 to 53,600 ppm.

Keywords: Membrane distillation; Water vapor flux; Water recovery; Module configuration

1. Introduction

With increasing demand for fresh water as well as recurring drought, desalination technologies have been developing rapidly. Low energy consumption and relatively smaller footprint make membrane-based techniques such as reverse osmosis (RO) and membrane distillation (MD) attractive alternatives [1–3]. Compared with thermal distillation, MD is a membrane-based evaporative process where the driving force is a temperature-induced vapor pressure difference caused by having a hot feed and a cold permeate [4]. Typically, MD is carried out at 60°C–90°C, which is significantly lower than conventional distillation [5–7]. Consequently, MD has the potential to generate high quality drinking water using low-grade heat such as waste heat from industrial processes and solar energy. The main efforts at improving MD performance have been aimed at the maximization of flux and salt rejection. Different types of membranes have been synthesized with improved porosity, optimized pore size distribution, incorporated nanomaterials and improved wetting and fouling resistance [8–13].

In spite of dramatic improvement in membrane properties, the overall mass recovery in MD remains quite low. This is a major drawback for MD and is a key roadblock towards commercialization [14,15]. A typical approach for the enhancement of water recovery in MD is to increase the membrane area or to put large numbers of modules in series or in parallel configurations [16–18]. However, it is important to note that MD is driven by the vapor pressure gradient which is a function of temperature, and maintaining the vapor pressure differential is of great importance. As water is evaporated through the membrane, the extraction of latent heat reduces the temperature on the feed side. Once the temperature or the vapor pressure differential is reduced, the increased area does not serve much purpose.

Efforts have been made to optimize MD performance. The performance of various MD configuration such as direct contact, vacuum, air gap and sweep gas has been evaluated at the laboratory as well as pilot plant scales, and heat and mass transport has been studied in details [5,15,19–30]. The dependence of module length on operating conditions, membrane thickness, recovery factor, the temperature and the flux profiles has been simulated to achieve seawater recovery factor of 70%. [31]. Lee et al. [32] described the cost-efficient desalination technology by integrating a countercurrent

* Corresponding author.

cascade of the novel cross-flow direct contact membrane distillation (DCMD) devices and solid polymeric hollow fiber-based heat exchange devices. The numerical simulator predicted a gained output ratio of 12 when unequal flow rates of the incoming brine and distillate streams are used [32]. Thermodynamic analysis of the DCMD system coupled with a heat exchanger has demonstrated that the process is mass-transfer limited and DCMD membrane area and permeability cannot be infinitely large [33,34].

Since it is not feasible to improve yield just by increasing membrane area alone, it is important to optimize module arrangements to maximize mass recovery factor. One could potentially think of multiple membrane modules in series and parallel configurations, some with heating stages in between to raise the temperature gradient before reintroduction to the next stage. The objective of this paper is to explore the different possible membrane module arrangements and study their effects on overall mass recovery.

2. Experimental

Polypropylene (PP) hollow fiber membrane module as well as flat sheet polytetrafluoroethylene (PTFE) membrane module were tested in this study [20,21]. Celgard X-20 PP hollow fibers (0.03 μm pores and 40% porosity, Celgard LLC, Charlotte, NC) and PTFE flat membrane from Advantec (0.2 μm pores and 70% porosity, Advantec MFS Inc.; Dublin, CA) were used for this study. The effective membrane area for the hollow fiber modules and the flat sheet membranes were 14.4 and 188 cm^2, respectively. The basic experimental setup has been described before [35–37] and shown in Fig. 1(a).

Different membrane module assemblies comprising of a set of two modules were tested in this study, and they are presented in Fig. 1(b). The respective module assemblies were as follows. two modules could be put in series where the hot brine leaving the first module entered the second one (MD-S). An alternate approach was to have two MD modules in series where the brine leaving the first module passes through a heat exchanger to regain the lost heat before entering the second module at a higher temperature and this was referred to as MD-SH. The two modules could also be put in parallel (MD-P). In simulating the multistage modular system, five smaller modules in MD-SH mode, a large module or the equivalent of MD-S, and five modules in MD-P are considered. The data are presented here for direct contact MD but can be utilized for any kind of MD, namely sweep gas membrane distillation (SGMD), DCMD and air gas membrane distillation (AGMD).

3. Results and discussions

3.1. Effect of feed temperatures and flow rates on water vapor flux

Fig. 2 shows the effect of feed temperature on water vapor flux for the two different membranes studied here. The water vapor flux increased with the increase in temperatures because increasing the feed temperature increases the vapor pressure and thereby increases the driving force. The water vapor flux increases with feed temperature exponentially, this is due to the associated exponential increase in the vapor pressure with temperature. As expected, the flux followed similar trends with the PTFE membrane showing significantly higher values at the same temperature.

Fig. 3 shows the effect of different module configuration on water vapor flux at various feed flow rates. Since inlet flow rates were kept the same, the total flow in the two modules in MD-P was double that of the MD-S or MD-SH. It is also observed from the figure that the overall flux increased with increase in flow rate. It was observed that with increase in the feed flow rate, the turbulence in the flow channel increases and hence the Reynolds number. This significantly improves the heat and mass transfer rates in the flow channels and leads to the reduction of the temperature and concentration polarization effect [35–40]. The higher feed flow rate also enhanced the average bulk temperature and consequently the temperature gradient across the membrane [38]. In Fig. 3, the influent temperature in each case was 80°C. The effluent temperatures from first module were around 60°C and 70°C for PP and PTFE membranes for all three modes. In MD-S, the effluent from module 1 was the influent to module 2, and the effluent from module 2 was at 48.6°C and 63°C, respectively, for PP and PTFE membranes. In MD-SH, the effluent water temperature from module 1 was reheated to 80°C before re-entering into the next module. It was observed from Figs. 2 and 3 that the overall water vapor flux was much lower for MD-S compared with MD-SH and MD-P because the temperature gradient in module 2 in this mode was much lower. Another contributing factor is that at low temperatures, the latent heat of evaporation was much higher and more energy was required to evaporate water [41].

Table 1 shows a comparison between all three configurations in terms of various DCMD performance parameters for PP and PTFE membranes. An enhancement in overall water vapor flux was 38% and 20% for MD-SH and MD-P in comparison with MD-S for PP and PTFE membrane, respectively. However, they also needed 11.7% and 27.21% more heat. In MD-P, the additional heat was supplied by heating more water and in MD-SH it was through the reheating before introduction to stage 2. Although, the MD-SH and MD-P showed similar water vapor flux and heat requirement, it is interesting to observe that the water recovery was much higher in MD-SH compared with MD-P. The mass recovery factor, defined as the percentage rate of permeate production per unit feed flow rate, was 1.9%, 2.6% and 1.3% in MD-S, MD-SH and MD-P, respectively. For the same amount of energy, the mass recovery factor was increased by 100% in MD-SH over MD-P. The trends were similar with the PTFE membrane.

3.2. Simulation of multi-stage membrane module system

Based on the above discussion, it is apparent that the configuration of the membrane modules is of great importance for optimizing MD especially from the standpoint of recovery. As already mentioned, the overall mass recovery factor cannot be increased effectively by just increasing the membrane area. In MD, the latent heat of evaporation for water vapor is obtained from the sensible heat of the circulating feed. For example, based on 80% efficiency, for a feed flow of 100 mL/min, the maximum available heat for vaporization at a temperature difference of 60°C (assuming inlet water temperature: 80°C and outlet water temperature: 20°C) is ~20 kJ/min. This heat is

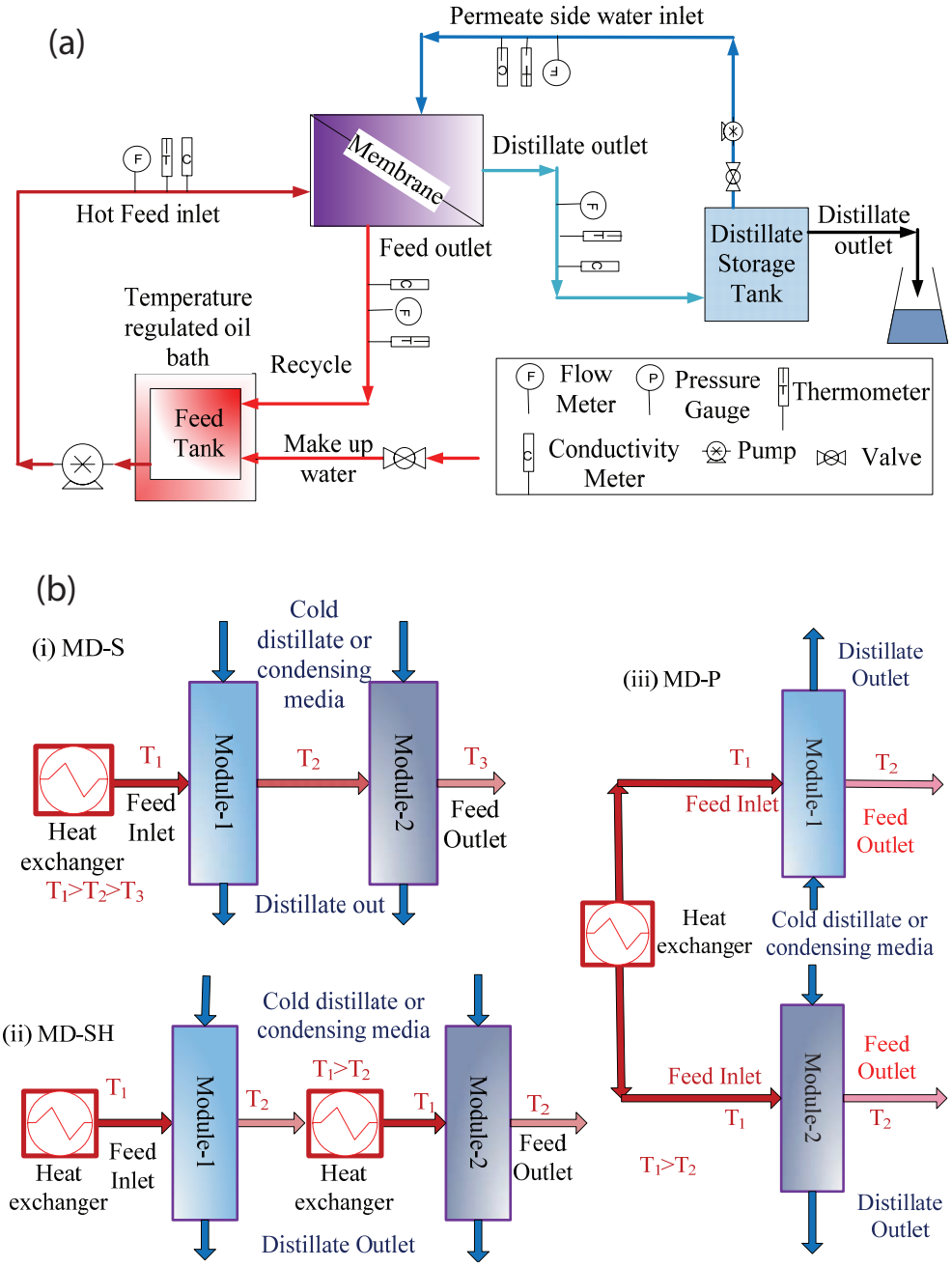

Fig. 1. (a) Schematic of the experimental setup. (b) Different MD configurations: (i) modules in series (MD-S), (ii) modules with in-between heating (MD-SH), (iii) modules in parallel (MD-P).

only enough to evaporate 8.7 mL/min water or 8.7% of feed. Considering a feed flow rate ~5 L/min, maximum 435 mL/min pure water generation is possible. For a membrane with a flux of 50 kg/m²h, the membrane area needed to generate this water would be no more than 0.52 m². Any additional membrane area would not enhance performance. The optimum membrane area will increase proportionally under equivalent conditions with increase in flow rate.

The above discussion serves as the basis for designing the number of stages needed for a certain mass recovery factor of pure water. The overall water recovery from a typical feed flow of 100 L/min is presented with five smaller modules in MD-SH mode, a large module or the equivalent of MD-S, and five modules in MD-P. In each case, the total membrane area is kept constant, the flux is assumed to be 50 kg/m² h; the feed inlet temperature is 80°C at a concentration of 34,000 ppm. The optimum area of a single module for conditions mentioned above is 10.44 m². Fig. 4 shows the MD-SH mode while MD-S and MD-P are similar to Fig. 1(b). In MD-SH, the effluent from each stage was reheated to 80°C before being reintroduced into the next module. The performances of the MD system for MD-SH, MD-P and a large module of equal

membrane area are presented in Tables 2 and 3. Since some water is removed at each stage, the subsequent membrane stage has a smaller membrane area.

Table 2 represents the performance data of individual modules of the MD-SH system. The membrane area was optimized based on the inlet feed flow rate. In Table 3, a comparative data of different system has been provided. It is clear from Tables 2 and 3 that a high water recovery of

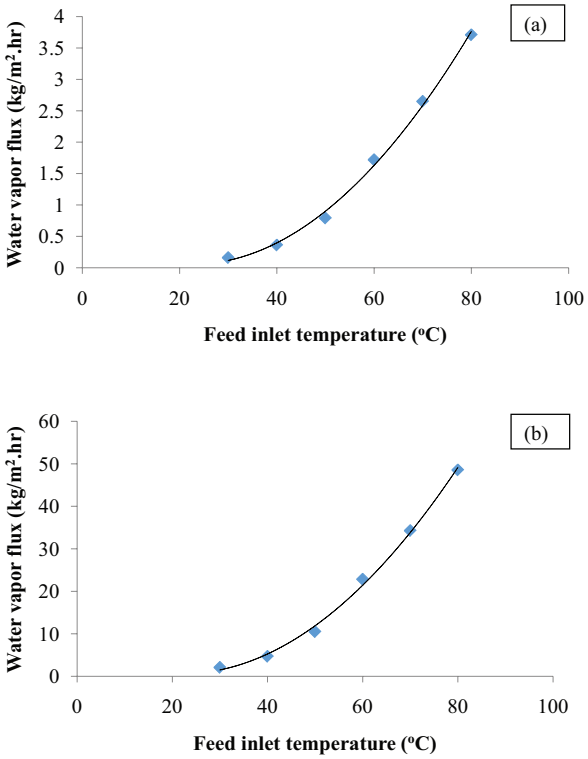

Fig. 2. Water vapor flux for (a) PP hollow fiber membrane and (b) flat PTFE membrane.

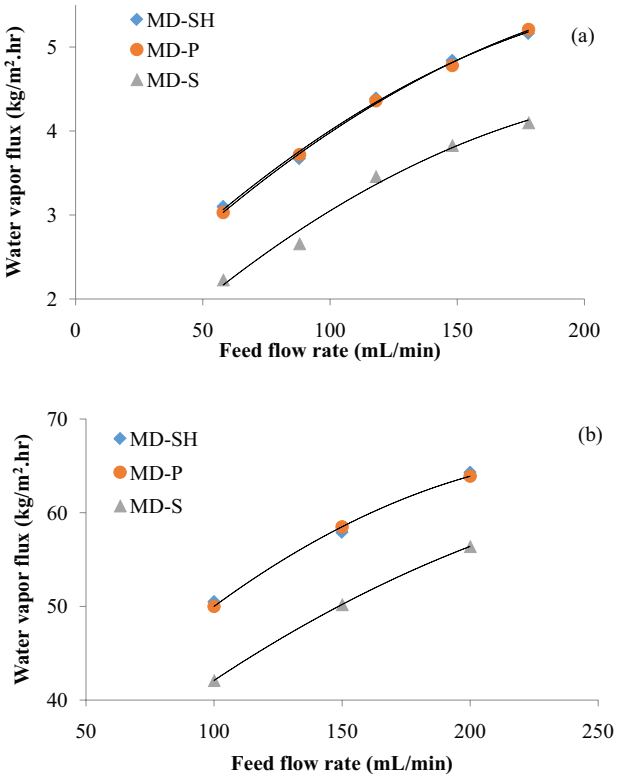

Fig. 3. Variation of water vapor flux at different flow rates for different configurations: (a) with PP hollow fiber modules and (b) with PTFE flat membrane modules at 80°C in MD-SH mode.

Table 1
Comparison between different module configurations with PP and PTFE modules at 80°C inlet temperature. The PP hollow fiber modules had an inlet flow rate of 88 mL/min and the PTFE module at 100 mL/min

Properties	PP			PTFE		
	MD-S	MD-SH	MD-P	MD-S	MD-SH	MD-P
Water vapor flux (kg/m² h)	2.66	3.67	3.72	42.1	50.5	50
Recovery from feed (%)	1.89	2.61	1.33	2.04	2.44	1.21
Total heat required (W)	120	134	134	196	242	242
Overall mass transfer coefficient (kg/m² s mmHg)	4.38E-06	6.04E-06	6.13E-06	6.93E-05	8.31E-05	8.23E-05

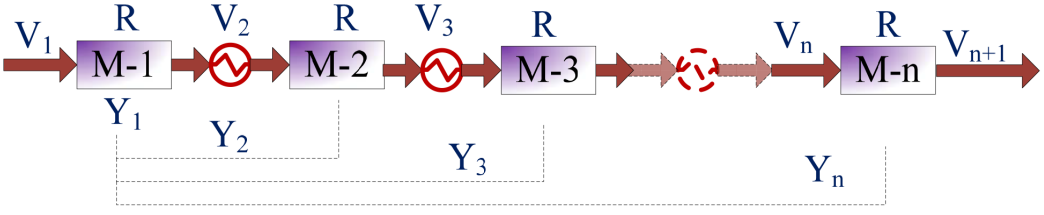

Fig. 4. Schematic of multi-stage MD with multiple modules..

Table 2
MD performance data of MD-SH

System	Feed (kg/h)		Membrane area (m^2)	Distillate collected (kg/h)	Recovery (%)	Salt concentration (ppm)	
	Inlet	Outlet				Inlet	Outlet
M-1	6,000	5,478	10.4	522	8.7	34,000	37,240
M-2	5,478	5,001	9.5	477	8.7	37,240	40,788
M-3	5,001	4,567	8.7	435	8.7	40,788	44,673
M-4	4,567	4,169	7.9	398	8.7	44,673	48,933
M-5	4,169	3,807	7.3	362	8.7	48,933	53,593
Overall	6,000	3,807	43.8	2,194	36.6	34,000	53,593

Table 3
Performance data with multi-modular system and comparison with single module

Membrane	Total membrane area (m^2)	Feed inlet (kg/min)	Water collected (kg/min)	Water recovery (%)	Heat required (kW)	Feed outlet concentration (ppm)
MD-SH	43.8	100	36.6	36.6	1,761	53,593
Large single module or MD-S	43.8	100	8.7	8.7	419	37.240
MD-P	43.8	500	36.5	7.3	1,765	36,677

~37% was obtained in MD-SH, and that was ~320% higher than that of a single large module or modules are in parallel. The percent water recovery was observed to be dependent on the number of modules in MD-SH system. The high recovery leads to the increase in salt concentration at each stage and the final outlet was also quite high around 53,593 ppm. On the other hand, for a large modular system and MD-P system, the water recovery was only 8.7% and the outlet salt rejection concentration was 37,240 ppm. It is clear from the simulated data that the multi-modular system with multi-stage heat exchangers between them is the most effective way of recovering large amount of water and also concentrating salt water.

The overall mass recovery factor of pure water in MD-SH depends upon the number of stages. As can be seen in Table 2, the total recovery with two modules was 16.6%, which increased to 36.6% with five modules and would further increase to 60% recovery with 10 stages. The overall mass recovery factor Y_n from n stages operated under the same conditions will be given by $Y_n = 1 - (1 - R)^n$, where R is the recovery at each stage. Therefore, the overall recovery can be increased by increasing the number of stages or R.

4. Conclusion

The overall water vapor recovery was higher in MD-SH configuration compared with MD-S and MD-P. Experiment using two stages of PP hollow fiber modules showed enhancements of 38% and 96% for MD-SH over MD-S and MD-P, respectively. The simulation with seawater with five stages in MD-SH mode showed 36.6% water recovery and the increase in brine concentration from 34,000 ppm at the influent to 53,600 ppm at the effluent. The recovery for MD-S and MD-P was 8.7% with exit salt concentrations of 37,240 and 36,700 ppm, respectively. Therefore, the solute preconcentration can be increased by increasing the number of stages in the MD-SH mode. Overall, the MD-SH leads to the optimum use of membrane area as well as energy usage for maximum water recovery.

Acknowledgment

The work was partially funded from a grant from the National Science Foundation (grant number CBET-1603314).

References

[1] B. Penate, L.G. Rodriguez, Current trends and future prospects in the design of seawater reverse osmosis desalination technology, Desalination, 284 (2012) 1–8.
[2] N. Misdan, W.J. Lau, A.F. Ismail, Seawater Reverse Osmosis (SWRO) desalination by thin-film composite membrane-current development, challenges and future prospects, Desalination, 287 (2012) 228–237.
[3] M. Li, Optimal plant operations of brackish water reverse osmosis (BWRO) desalination, Desalination, 293 (2012) 61–68.
[4] P. Peng, A.G. Fane, X. Li, Desalination by membrane distillation adopting a hydrophilic membrane, Desalination, 173 (2005) 45–54.
[5] F.A. Banat, F.A.A. Al-rub, R. Jumah, A. Al-Shannag, Modeling of desalination using tubular direct contact membrane distillation modules, Sep. Sci. Technol., 34 (1999) 2191–2206.
[6] F.A. Banat, F.A. Al-Rub, R. Jumah, M. Shannag, On the effect of inert gases in breaking the formic acid–water azeotrope by gas-gap membrane distillation, Chem. Eng. J., 73 (1999) 37–42.
[7] F.A. Banat, F.A. Al-Rub, M. Shannag, Simultaneous removal of acetone and ethanol from aqueous solutions by membrane distillation: prediction using the Fick's and the exact and approximate Stefan-Maxwell relations, Heat Mass Transfer, 35 (1999) 423–431.
[8] P. Wang, T. Chung, Recent advances in membrane distillation processes: membrane development, configuration design and application exploring, J. Membr. Sci., 474 (2015) 39–56.
[9] S. Ragunath, S. Roy, S. Mitra, Selective hydrophilization of the permeate surface to enhance flux in membrane distillation, Sep. Purif. Technol., 170 (2016) 427–433.
[10] M. Bhadra, S. Roy, S. Mitra, A bilayered structure comprised of functionalized carbon nanotubes for desalination by membrane distillation, ACS Appl. Mater. Interfaces, 8 (2016) 19507–19513.

[11] M. Bhadra, S. Roy, S. Mitra, Flux enhancement in direct contact membrane distillation by implementing carbon nanotube immobilized PTFE membrane, Sep. Purif. Technol., 161 (2016) 136–143.
[12] M. Gryta, The study of performance of polyethylene chlorinetrifluoroethylene membranes used for brine desalination by membrane distillation, Desalination, 398 (2016) 52–63.
[13] M. Essalhi, M. Khayet, Self-sustained webs of polyvinylidene fluoride electrospun nano-fibers: effects of polymer concentration and desalination by direct contact membrane distillation, J. Membr. Sci., 454 (2014) 133–143.
[14] X. Yang, R. Wang, A.G. Fane, C.Y. Tang, I.G. Wenten, Membrane module design and dynamic shear-induced techniques to enhance liquid separation by hollow fiber modules: a review, Desal. Wat. Treat., 51 (2013) 3604–3627.
[15] E. Drioli, A. Ali, F. Macedonio, Membrane distillation: recent developments and perspectives, Desalination, 356 (2015) 56–84.
[16] E. Guillén-Burrieza, J. Blanco, G. Zaragoza, D.-C. Alarcón, P. Palenzuela, M. Ibarra, W. Gernjak, Experimental analysis of an air gap membrane distillation solar desalination pilot system, J. Membr. Sci., 379 (2011) 386–396.
[17] J.-G. Lee, W.-S. Kim, Numerical study on multi-stage vacuum membrane distillation with economic evaluation, Desalination, 339 (2014) 54–67.
[18] M.W. Shahzad, M. Burhan, K.C. Ng, Pushing desalination recovery to the maximum limit: membrane and thermal processes integration, Desalination, 416 (2017) 54–64.
[19] F.A. Banat, F.A. Al-Rub, R. Jumah, M. Shannag, Theoretical investigation of membrane distillation role in breaking the formic acid-water azeotropic point: comparison between Fickian and Stefan-Maxwell-based models, Int. Commun. Heat Mass Transfer, 26 (1999) 879–888.
[20] F.A. Banat, F.A. Al-Rub, R. Jumah, M. Shannag, Application of Stefan–Maxwell approach to azeotropic separation by membrane distillation, Chem. Eng. J., 73 (1999) 71–75.
[21] F.A. Al-Rub, F.A. Banat, M. Shannag, Theoretical assessment of dilute acetone removal from aqueous streams by membrane distillation, Sep. Sci. Technol., 34 (1999) 2817–2836.
[22] I. Hitsov, T. Maere, K. De Sitter, C. Dotremont, I. Nopens, Modelling approaches in membrane distillation: a critical review, Sep. Purif. Technol., 142 (2015) 48–64.
[23] J.-G. Lee, E.-J. Lee, S. Jeong, J. Guo, A.K. An, H. Guo, J. Kim, T. Leiknes, N. Ghaffour, Theoretical modeling and experimental validation of transport and separation properties of carbon nanotube electrospun membrane distillation, J. Membr. Sci., 526 (2017) 395–408.
[24] S. Alobaidani, E. Curcio, F. Macedonio, G. Diprofio, H. Alhinai, E. Drioli, Potential of membrane distillation in seawater desalination: thermal efficiency, sensitivity study and cost estimation, J. Membr. Sci., 323 (2008) 85–98.
[25] A. Hausmann, P. Sanciolo, T. Vasiljevic, U. Kulozik, M. Duke, Performance assessment of membrane distillation for skim milk and whey processing, J. Dairy Sci., 97 (2014) 56–71.
[26] F. Macedonio, A. Ali, T. Poerio, E. El-sayed, E. Drioli, M. Abdel-Jawad, Direct contact membrane distillation for treatment of oilfield produced water, Sep. Purif. Technol., 126 (2014) 69–81.
[27] D. Winter, J. Koschikowski, S. Ripperger, Desalination using membrane distillation: flux enhancement by feed water deaeration on spiral-wound modules, J. Membr. Sci., 423–424 (2012) 215–224.
[28] L. Francis, N. Ghaffour, A.A. Alsaadi, G.L. Amy, Material gap membrane distillation: a new design for water vapor flux enhancement, J. Membr. Sci., 448 (2013) 240–247.
[29] K. Zhao, W. Heinzl, M. Wenzel, S. Büttner, F. Bollen, G. Lange, S. Heinzl, N. Sarda, Experimental study of the memsys vacuum-multi-effect-membrane-distillation (V-MEMD) module, Desalination, 323 (2013) 150–160.
[30] L. Camacho, L. Dumée, J. Zhang, J. Li, M. Duke, J. Gomez, S. Gray, Advances in membrane distillation for water desalination and purification applications, Water, 5 (2013) 94–196.
[31] A. Ali, C.A. Quist-Jensen, F. Macedonio, E. Drioli, Optimization of module length for continuous direct contact membrane distillation process, Chem. Eng. Process. Process Intensif., 110 (2016) 188.
[32] H. Lee, F. He, L. Song, J. Gilron, K.K. Sirkar, Desalination with a cascade of cross-flow hollow fiber membrane distillation devices integrated with a heat exchanger, AIChE J., 57 (2011) 1780–1795.
[33] S. Lin, N.Y. Yip, M. Elimelech, Direct contact membrane distillation with heat recovery: thermodynamic insights from module scale modeling, J. Membr. Sci., 453 (2014) 498.
[34] H. Yu, X. Yang, R. Wang, A.G. Fane, Numerical simulation of heat and mass transfer in direct membrane distillation in a hollow fiber module with laminar flow, J. Membr. Sci., 384 (2011) 107.
[35] M. Bhadra, S. Roy, S. Mitra, Desalination across a graphene oxide membrane via direct contact membrane distillation, Desalination, 378 (2016) 37–43.
[36] M. Bhadra, S. Roy, S. Mitra, Enhanced desalination using carboxylated carbon nanotube immobilized membranes, Sep. Purif. Technol., 120 (2013) 373–377.
[37] S. Roy, M. Bhadra, S. Mitra, Enhanced desalination via functionalized carbon nanotube immobilized membrane in direct contact membrane distillation, Sep. Purif. Technol., 136 (2014) 58–65.
[38] F. Mahmoudi, G.M. Goodarzi, S. Dehghani, A. Akbarzadeh, Experimental and theoretical study of a lab scale permeate gap membrane distillation setup for desalination. Desalination, 419 (2017) 197–210.
[39] L. Li, K.K. Sirkar, Studies in vacuum membrane distillation with flat membranes, J. Membr. Sci., 523 (2017) 225–234.
[40] M.E. Leitch, G.V. Lowry, M.S. Mauter, Characterizing convective heat transfer coefficients in membrane distillation cassettes, J. Membr. Sci., 538 (2017) 108–121.
[41] G. Narsimhan, Temperature dependence of latent heat of vaporization, J. Phys. Chem., 67 (1963) 2238.